



UNIVERSITY OF LEEDS

This is a repository copy of *Catalysis in flow: Operando study of Pd catalyst speciation and leaching*.

White Rose Research Online URL for this paper:
<http://eprints.whiterose.ac.uk/84124/>

Version: Accepted Version

Article:

Brazier, JB, Nguyen, BN, Adrio, LA et al. (6 more authors) (2014) Catalysis in flow: Operando study of Pd catalyst speciation and leaching. *Catalysis Today*, 229. 95 - 103. ISSN 0920-5861

<https://doi.org/10.1016/j.cattod.2013.10.079>

Reuse

Items deposited in White Rose Research Online are protected by copyright, with all rights reserved unless indicated otherwise. They may be downloaded and/or printed for private study, or other acts as permitted by national copyright laws. The publisher or other rights holders may allow further reproduction and re-use of the full text version. This is indicated by the licence information on the White Rose Research Online record for the item.

Takedown

If you consider content in White Rose Research Online to be in breach of UK law, please notify us by emailing eprints@whiterose.ac.uk including the URL of the record and the reason for the withdrawal request.



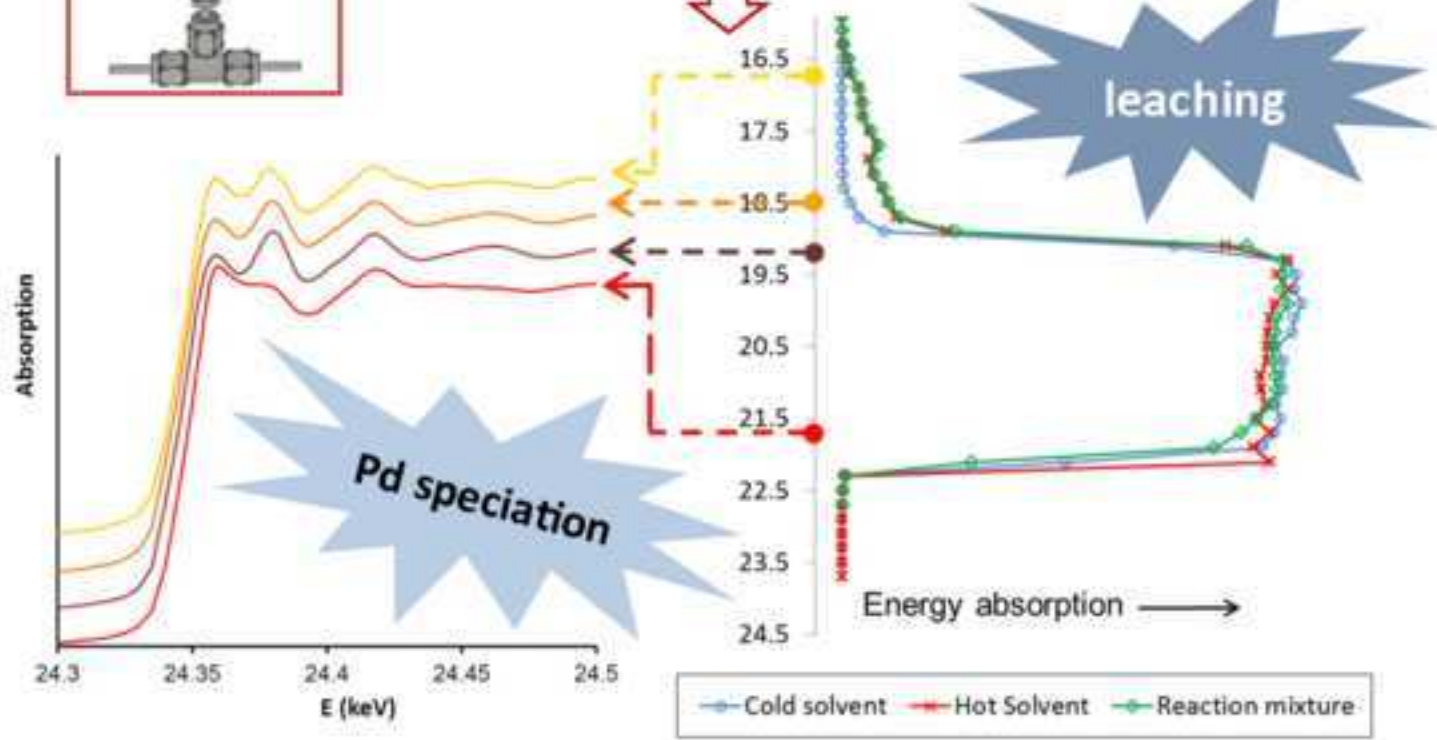
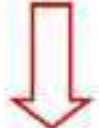
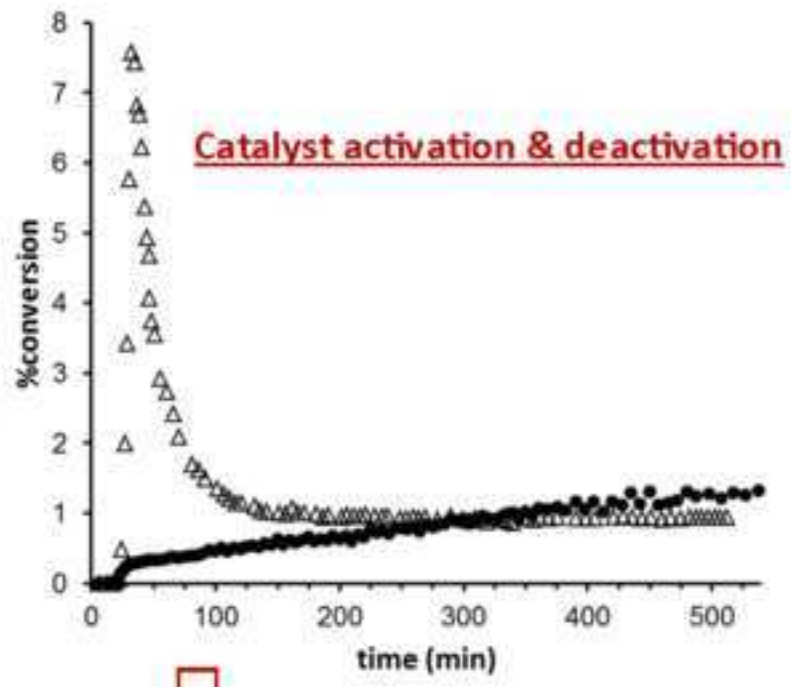
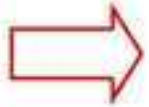
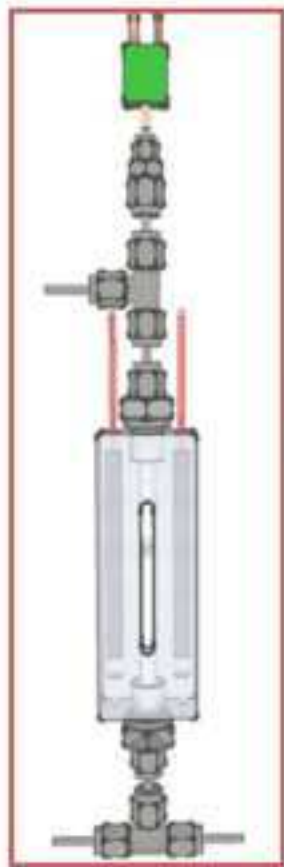
eprints@whiterose.ac.uk
<https://eprints.whiterose.ac.uk/>

Catalysis in Flow: Operando study of Pd catalyst speciation and leaching.

John B. Brazier,^a Bao N. Nguyen,^{a,†} Luis A. Adrio,^{a,§} Elena M. Barreiro,^a Wai Peng Leong,^a Mark A. Newton,^c Santiago J. A. Figueroa,^{c,‡} Klaus Hellgardt,^{b,*} and King Kuok (Mimi) Hii^{a,*}

Highlights:

- A custom-made plug-flow reactor (PFR) was constructed for examining Pd catalysis
- Leaching/reaction profiles of two Pd catalysts for the Suzuki-Miyaura reaction were established by filtration studies.
- The PFR was used to examine catalyst activation and deactivation processes
- Ethanol was found to affect the catalysts differently
- Leaching and speciation of Pd along the catalyst bed has been observed for the very first time.



Catalysis in Flow: Operando study of Pd catalyst speciation and leaching.

John B. Brazier,^a Bao N. Nguyen,^{a,†} Luis A. Adrio,^{a,§} Elena M. Barreiro,^a Wai Peng Leong,^a Mark A. Newton,^c Santiago J. A. Figueroa,^{c,¶} Klaus Hellgardt,^{b,*} and King Kuok (Mimi) Hii^{a,*}

^aDepartment of Chemistry and ^bDepartment of Chemical Engineering, Imperial College London, South Kensington, London SW7 2AZ, U.K. ^cEuropean Synchrotron Radiation Facility (ESRF), 6 rue Jules Horowitz, 38000, Grenoble, France.

Abstract: A custom-made plug-flow reactor was designed and constructed to examine the behaviour of Pd catalysts during Suzuki-Miyaura cross-coupling reactions. Spatial-temporal resolution of catalyst activation, deactivation and leaching processes can be obtained by single-pass experiments. Subsequent deployment of the flow reactor in a XAS beam line revealed speciation of Pd along the catalyst bed.

1. Introduction

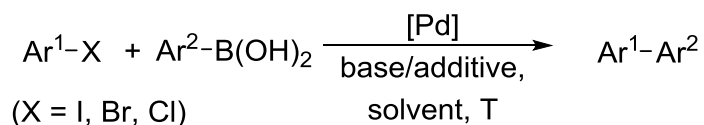


Figure 1. The Suzuki-Miyaura reaction.

The Suzuki-Miyaura reaction (Figure 1) is one of the most powerful methods for construction of aryl-aryl bonds and has been the subject of intensive research over the last few decades.[1] Despite its widespread popularity in many industrial processes, the identity of the catalytically active species remains a hotly debated, yet unresolved, topic in chemistry. In some cases, catalytic turnovers with aryl iodide and bromide substrates (X = I, Br) can be achieved at room temperature under ‘ligandless’ conditions using simple palladium(II) salts such as Pd(OAc)₂[2] or supported Pd/C[3] as catalyst precursors. There appears to be a general consensus that, in some cases, catalysis is a result of Pd leached into solution facilitating a (quasi-) homogeneous reaction, however, contributions from surface-catalyzed reaction cannot be entirely ruled out.[4]

Accordingly, there are an increasing number of in situ and operando experimental tools used to interrogate the Suzuki-Miyaura reactions at different length scales – ranging from global responses by kinetic measurements[5] to observation of surface and solution species by spectroscopic methods,

including XAS[6, 7] and STEM/HRTEM imaging[8] techniques. Previously, operando X-ray absorption spectroscopy (XAS) studies have been conducted on Pd catalysts in a Suzuki-Miyaura[6] and closely related Heck reactions:[9] Lee and co-workers employed a reactor cell to recirculate a solution of the catalyst under study (PVP-stabilised Pd nanoparticles) through the path of the X-ray beam during data acquisition. On the other hand, Grunwaldt, Baiker and co-workers constructed a batch cell reactor with two separate X-ray transparent windows, allowing the liquid phase and the catalyst bed of Pd/Al₂O₃ to be examined. In both of these studies, relatively long acquisition times were required, which impose certain limitations on these methods.

Fixed-bed plug flow reactors (PFR's) are commonly employed in XAS for studying gas-phase reactions over heterogeneous catalysts under high temperature and pressure.[10] The reactor is typically mounted in a beam line such that the X-ray beam passes across the bed at a specific position, or, in one example, axially along the catalyst bed.[11] In the former arrangement, only changes in the catalyst at a fixed position can be examined, while in the latter, any gradients in the catalyst bed will be averaged.

In a PFR, product conversion is dictated by residence time in the catalyst bed. At steady-state, a concentration gradient is present along the length of the catalyst bed. If no changes to catalyst or leaching occur, the single-pass output of the reaction stream should remain constant over time.

Conversely, leaching or catalyst deactivation is expected to affect the metal's composition along the catalyst bed, with concurrent changes in single-pass conversions. Using an X-ray beam, it should be possible to interrogate the structure of the catalyst at different positions, which can be directly correlated to specific residence times and product output. Thus, structural-activity relationships can be established temporally and spatially, in a way that is not possible to achieve by the aforementioned batch reactors. Herein, the construction and characterisation of such a continuous flow reactor is described, which was used to study the speciation and leaching of Pd catalysts under operando conditions in Suzuki-Miyaura reactions.

2. Material and methods

2.1 Description of the flow reactor

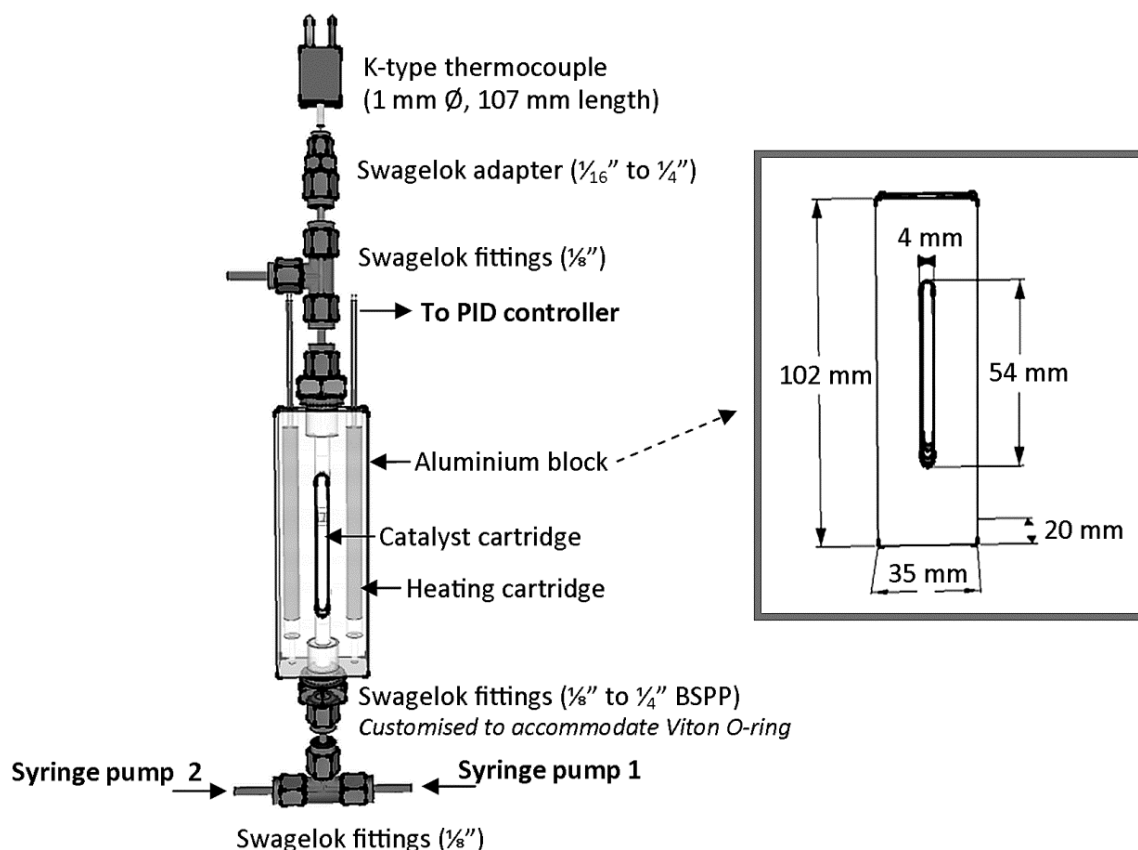


Figure 2. Design and setup of the plug flow reactor.

2.1.1 Design (Figure 2). The continuous plug flow reactor consists of an aluminium block with drilled cylindrical bores to accommodate a catalyst cartridge (4 mm inner \varnothing , 1 mm wall thickness, either quartz or perfluoroalkoxy, 'PFA', fluoropolymer) and cartridge heaters (1/4" x 3", Under Control Instruments Ltd) powered and controlled with a PID controller (Sesto D1S-VR-200). Parallel slits (4 x 54 mm) in the aluminium heating block provide a path of transmission for X-ray studies. A liquid-tight seal at each end of the catalyst cartridge was achieved by compression of two Viton O-rings (5 mm i.d., 1 mm cross-section) by Swagelok fittings. The top of the reactor was connected to an outlet with a K-type thermocouple positioned to measure the temperature of the eluent as it exited the catalyst cartridge (RS-53II digital thermometer connected to PC); at the bottom, a T-piece (the mixing junction) connected to two syringe pumps (Graseby 3200) to deliver solvent or reaction mixture to the reactor. Another K-type thermometer is fitted to the side (not shown) to provide a feed-back loop to the PID controller.

2.1.2 Heating characteristics. 50% aq. EtOH was passed through a catalyst cartridge at 0.1 mL/min. With the temperature of the effluent monitored at the exit of the cartridge, the reactor was heated to 80 °C (set temperature), during which thermal images were recorded at regular time intervals using a Testo 880 infra-red camera, with concomitant monitoring of the eluent temperature at the top of the

reactor. Results of the experiment are provided in the text (vide infra) and as Supplementary Material (Figures S2, S3 and associated text).

2.1.3 Tracer experiments. The reactor was fitted with a cartridge that was either empty, or packed with quartz sand and alumina (described in section 2.2.2). The syringe pumps were loaded with syringes containing solvent (50% aq. ethanol), or a solution of the tracer (20 mM of 4-hydroxyacetophenone in 50% aq. EtOH) and connected to the reactor. At the beginning of the experiment, the reactor assembly was heated at 80 °C and flushed with 50% aq. ethanol using syringe pump 1. After 15 min, syringe pump 1 was switched off while syringe pump 2 containing the tracer was switched on at 0.1 mL/min simultaneously. Eluting fractions were collected every 2 min (Pharmacia LKB fraction collector), and analysed by HPLC (see section 2.3).

2.2 Catalysts

Pd EncatTM 30NP (0.4 mmol/g) catalyst was procured from Sigma-Aldrich and used as received.

2.2.1 Preparation of Pd/ γ -Al₂O₃. [12] In a 250 mL Erlenmeyer flask, γ -aluminium oxide (9.5 g) was suspended in distilled water (125 mL) and a solution of PdCl₂ (0.83 g) dissolved in 5% aq. HCl (25 mL) was added with magnetic stirring (500 rpm). The pH of the suspension was subsequently adjusted to pH 10 over a period of ca. 50 min, by the addition of 10% aq. NaOH using a syringe pump (set at flow rate 18 mL/h) connected to a pH controller. Stirring was then continued for a further 1 h, before the slurry was filtered. The collected catalyst was washed twice with distilled water and dried in a vacuum desiccator at room temperature overnight ('dried'). A portion of the catalyst was calcined in a furnace, raising the temperature from ambient to 500 °C over 4 hours, and maintaining it for 500 °C for a further two hours before cooling back to room temperature ('calcined'). ICP analysis revealed catalytic loading of 4.5 wt% Pd. The preparation was repeated, doubling the amount of the PdCl₂ precursor, to furnish a sample with 8 wt% Pd.

2.2.2 Packing of the catalyst cartridge (Figure 3). A clean tube was mounted vertically in a socket connected to a vacuum line. Cotton wool was introduced to create a small plug (ca. 17 mm, 30 mg) at the bottom of the tube, and a light vacuum was applied. Layers of quartz sand (50-70 mesh, 20 mm, ca. 300 mg), γ -alumina (Alfa Aesar, 40-80 nm, 180 m²/g, 2 mm, ca. 8 mg), Pd/ γ -Al₂O₃ (particle size <80 μ m) or Pd EncatTM 30NP (ca. 3.5 mm, 30 mg), γ -alumina (1.5 mm, ca. 6 mm) and quartz sand (39 mm, ca. 550 mg) were introduced successively, taking care to flatten each surface with a metal rod. The tube was sealed with another plug of cotton wool (ca. 17 mm, 30 mg). The cartridge was mounted in the reactor such that the direction of reactant flow is aligned in the direction in which vacuum was applied, so as to minimise loosening/movement of the layers.

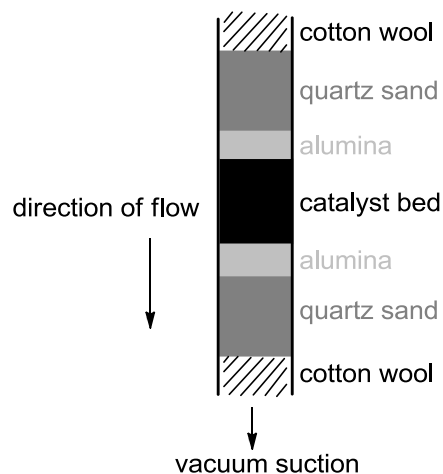


Figure 3. Packing of the catalyst cartridge.

2.3 Catalytic reactions

Glassware were treated with aqua regia ($\text{HNO}_3\text{:HCl}$, 1:3 v/v), rinsed thoroughly with water and dried in an oven prior to use. Unless otherwise stated, catalytic reactions were analysed by using an HP1050 HPLC system fitted with a Gemini NX-C18 $5\mu\text{m}$ 110A column (Phenomenex, 250 x 4.6 mm), with UV detection at 220 nm. The column was eluted with a solution comprising 72.5% methanol and 27.5% phosphoric acid (0.85%) at 1 mL/min.

2.3.1 Evaluation of catalyst leaching in aliquot: A 100 mL round bottomed flask was charged with 2-bromoanisole **1** (607 mg, 0.406 mL, 3.2 mmol, 1 eq.), 4-fluorophenylboronic acid **2** (500 mg, 3.6 mmol, 1.1 eq.), K_3PO_4 (690 mg, 3.2 mmol, 1 eq.) and 30 mg of 4.5% Pd/ $\gamma\text{-Al}_2\text{O}_3$ (dried) or Pd EncatTM 30NP (0.4 mmol/g). A mixture of ethanol–water (1:1 v/v, 65 mL) was then added and the reaction mixture was stirred at 75 °C until completion (3 h, total conversion of the reactant to product was confirmed by ^1H NMR spectroscopy). The reaction mixture was cooled to room temperature and then filtered through filter paper (VWR qualitative filter 413, pore size 5-13 μm). The filtrate was transferred to a clean round-bottom flask charged with further portions of 4-bromoacetophenone **4** (647 mg, 3.2 mmol, 1 eq.), 4-fluorophenylboronic acid **2** (500 mg, 3.6 mmol, 1.1 eq.) and K_3PO_4 (690 mg, 3.2 mmol, 1 eq.). The mixture was stirred at 75 °C. Product conversion was assessed after 2 h by TLC and ^1H NMR (Supplementary Material).

2.3.2 Evaluation of catalyst pre-treatment by ethanol: A 2-necked 100 mL round-bottom flask was purged with dry N_2 , and charged with a mixture of 4-bromoacetophenone **4** (647 mg, 3.2 mmol, 1 eq.), (4-fluorophenyl)boronic acid **2** (500 mg, 3.6 mmol, 1.1 eq.) and K_3PO_4 (690 mg, 3.2 mmol, 1 eq.) in ethanol–water (1:1 v/v, 50 mL). The solution was warmed up to 75 °C before the catalyst was added (30 mg of 4.5% Pd/ $\gamma\text{-Al}_2\text{O}_3$ (dried) or Pd EncatTM 30NP). Product formation was determined by HPLC

analysis. In a separate experiment, the catalyst was subjected to heating in a mixture of aq. ethanol (1:1 v/v, 20 mL) for 2 hours at 75 °C. After cooling, the solvent was removed by syringe, before the addition of a pre-mixed solution of 4-bromoacetophenone **4** (647 mg, 3.2 mmol, 1 eq.), (4-fluorophenyl)boronic acid **2** (500 mg, 3.6 mmol, 1.1 eq.), K₃PO₄ (690 mg, 3.2 mmol, 1 eq.) in aq. ethanol (1:1 v/v, 50 mL). The solution was stirred at 75°C and the product formation was determined by HPLC analysis.

2.3.3 Single-pass experiments: A catalyst cartridge was prepared and mounted into the flow reactor. A 60-mL syringe was filled with 50% aqueous ethanol, loaded into the solvent syringe pump (#1) and connected to the apparatus. The solvent delivery line was flushed through with solvent. 4-Bromoacetophenone (647 mg, 3.25 mmol), 4-fluorobenzeneboronic acid (500 mg, 3.57 mmol) and potassium phosphate (690 mg, 3.25 mmol) were dissolved in 50% aqueous ethanol (65 mL). The solution was drawn up into a 60-mL syringe which was mounted into the reagent syringe pump (#2), and the reagent delivery line was flushed through with the reagent solution.

Both the solvent and solution delivery lines were attached to the reactor via the mixing junction for single pass-experiments. Pre-treatment of the catalyst with solvent: The reactor was initially flushed through with solvent (syringe pump #1) at a flow rate of 0.1 mL/min. The flow rate was then reduced to 0.05 mL/min, before the temperature was raised to 80 °C. A solvent flow of 0.05 mL/min was maintained for 18 h. At the end of this period, the solvent pump was turned off and the reagent pump turned on (time t=0) to deliver the reaction mixture to the catalyst cartridge at 0.1 mL/min. The eluent was collected using a fraction collector (Pharmacia LKB fraction collector).

2.4 XAS studies

QuEXAFS and scanning EXAFS experiments were performed at the BM23 beam line located at ESRF, Grenoble, France. The reactor system was mounted on a Huber motor to facilitate x-y-z motion and thus fast scanning of the catalyst packing during operation. Syringe pumps were replaced by Nexus 6000 and a EuroTherm94c was used as the PID controller, such that the temperature and flow rates can be controlled remotely via RS232 interfaces, to allow for changes of operating conditions during continuous observation.

QuEXAFS measurements were made with a Si (111) fixed exit double crystal monochromator providing an X-ray beam spot size of ca. 0.2 mm vertical x 2 mm horizontal bidirectional QuEXAFS (as described in [13]) was collected over an energy range of 24 to 25.365 keV with each scan, taking 6 seconds. Three ionisation chambers were used for to collect X-ray reference (I₀), sample (I_s) and Pd foil simultaneously.

3. Results and Discussion

3.1 Design and construction of the fixed-bed plug flow reactor.

A laboratory-scale fixed bed plug flow reactor was specifically constructed for time-resolved study of heterogeneous catalysis (Figure 2). Quartz and PFA cartridges were chosen for their good mechanical and thermal stability towards aqueous alcoholic solvents at the operating temperature (typically 75 °C), whilst also providing a transparent window for X-ray spectroscopic studies of second row transition metal catalysts (Y K-edge: 17038 eV).

The reactor's heat and flow profiles were established to ensure reproducibility of results, so as to allow for consistency in subsequent kinetic analysis and modelling. Heating of the catalyst bed was achieved by cartridge heaters inserted within the aluminum block, regulated by a PID controller. Heating is very rapid; the eluent from the reactor reaches 75 °C (stable temperature) in under 10 min at the catalyst cartridge exit. In order to determine the presence of any irregular heating patterns within the catalyst cartridge, a thermal camera was employed to monitor heating of the cartridge under flowing solvent (Figure 4 and [supplementary video here](#)). No thermal hotspots or gradients were detected within the catalyst cartridge during heating, confirming that even (isothermal) temperature distribution can be achieved.

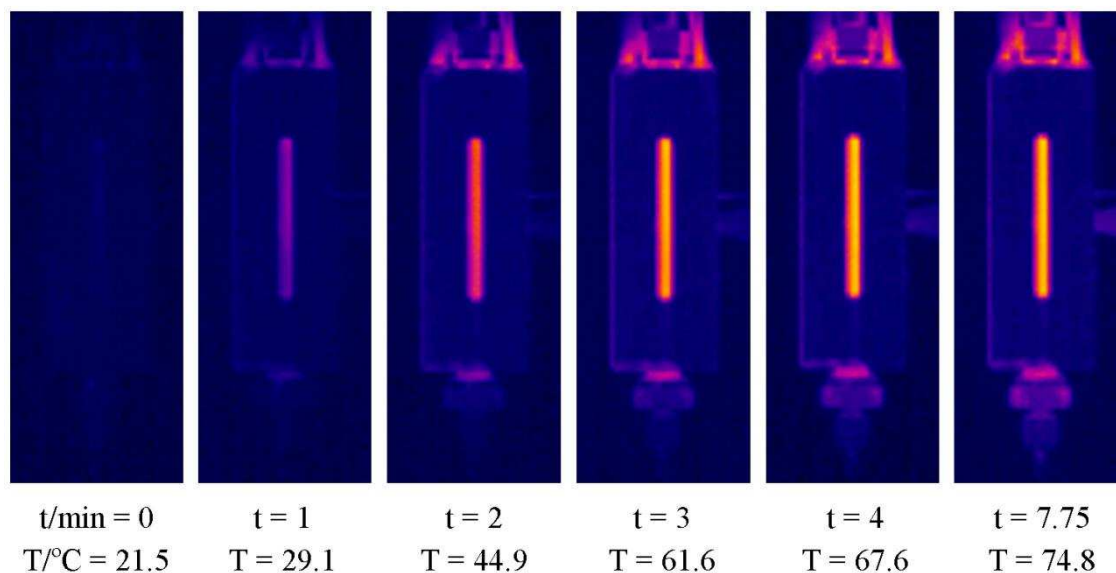


Figure 4. Heating profile of the catalyst cartridge established by thermal imaging. Temperature recorded of the eluent at the exit.

In order for catalyst speciation to be observable, it is critical for the reactor to function effectively as a PFR, such that at any given cross-section, the palladium catalyst is exposed to the same amount of reactants, i.e. the reaction stream flows through the cartridge at the same velocity in parallel, so that the

fluid is perfectly mixed radially without axial back-mixing (low ‘dispersion’). With this in mind, syringe pumps were used to deliver a continuous non-oscillating flow of solvent or reaction mixture to minimise flow fluctuations within the reactor system. Dispersion effects are further minimised by judicious elimination of fittings and changes in flow path diameter.

The mixing characteristics of empty and packed catalyst cartridges were established by tracer experiments: a solution of 4-acetylphenol was delivered into the reactor at the same rate as single-pass experiments (0.1 mL/min), while the outlet stream was monitored as a function of time. As expected (Figure 5), the empty cartridge exhibits significant dispersion, which sharpens in the presence of a packed cartridge. Subsequently, a simple tanks-in-series model was developed in Berkley Madonna software (<http://www.berkeleymadonna.com/>), in order to fit the experimental data of the tracer experiments carried out with the empty and packed cartridges. The step response for the empty cartridge could be modelled with a tanks-in-series model involving 1.8 CSTRs (Figure 5A) whereas the packed cartridge resulted in a best fit using 6.7 CSTRs (Figure 5B).

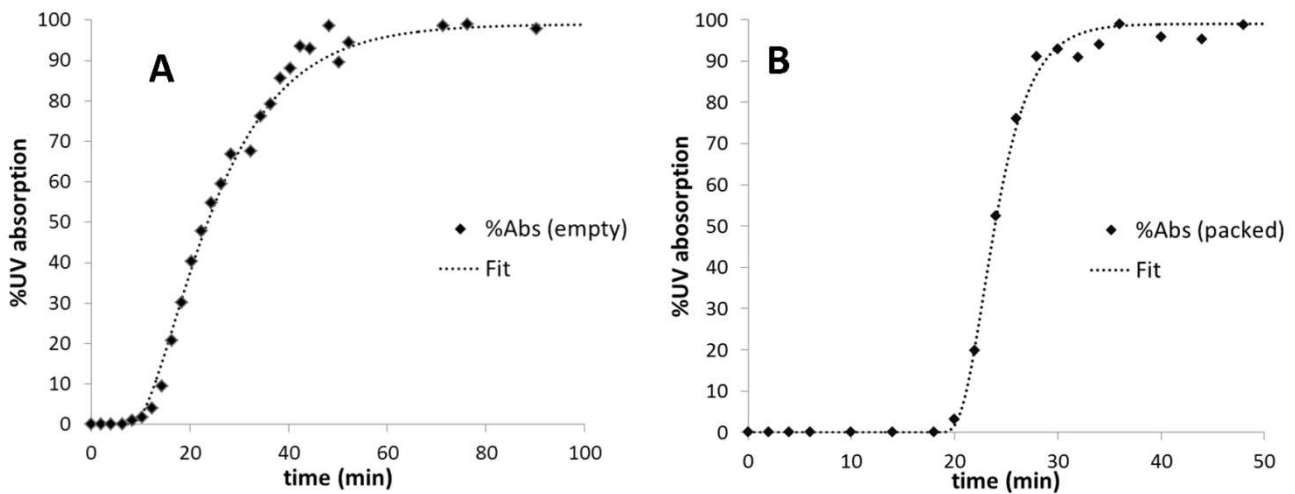


Figure 5. Tracer experiments: **A** = Empty cartridge; **B** = Packed cartridge.

These data in turn result in variances σ_{θ}^2 of 0.55 and 0.15, respectively using the following, simple relationship:

$$\sigma_{\theta}^2 = \frac{1}{N} \quad (\text{Eqn.1})$$

where N is the number of CSTRs in series required to fit the response of the reactor system to a step change in tracer concentration.

The variance, in turn, can also be developed as a function of the Peclet number (Pe , understood here to be the axial Peclet number) (Eqn. 2), usually derived for a pulse response. Irrespective of the derivation, this equation for the variance can be solved for the axial reactor Pe number (2.13 and 12.2, respectively) and subsequently for the molecular dispersion number (D_e):

$$\sigma_{\theta}^2 = \frac{2}{Pe} \left[1 - \frac{1}{Pe} (1 - e^{-Pe}) \right] \quad (\text{Eqn.2})$$

with

$$Pe = \frac{uL}{D_e} \quad (\text{Eqn.3})$$

where

$$u = 2.09 \cdot 10^{-6} \text{ m s}^{-1}$$

L = particle diameter d_p (10^{-4} m) for packed bed and tube diameter d_t ($4 \cdot 10^{-3}$ m) for empty tube

A dispersion number of $3.93 \cdot 10^{-9} \text{ m}^2 \text{ s}^{-1}$ is thus calculated for the empty cartridge and $6.86 \cdot 10^{-12} \text{ m}^2 \text{ s}^{-1}$ for the packed catalyst bed, respectively.

Given the low D_e and Pe of >10 , the (packed) catalyst cartridge may be treated effectively as a plug flow reactor (PFR) in subsequent modelling analysis.

3.2 Choice of catalyst and leaching study.

4.5% Pd/ γ - Al_2O_3 (dried) and Pd EncatTM 30NP were chosen for our preliminary study. The alumina-supported catalyst is active for Suzuki-Miyaura coupling of aryl bromides and certain chlorides, and its activity has been attributed to leached palladium species.[12] In contrast, Pd EncatTM 30NP uses microencapsulation technology to incarcerate Pd-nanoparticles within a polyurea matrix. It was reported to catalyse cross-coupling between aryl bromides and arylboronic acids up to 4 times without any loss in catalyst activity, and Pd leaching was reported to be ‘extremely low’ (0.2% after 4 cycles).[14] Even so, the involvement of soluble, catalytically active Pd species cannot be ruled out entirely,[15, 16] as it is known that Suzuki-Miyaura reactions can be catalysed by ppb-levels of Pd.[17]

In this work, the catalyst activity and leaching profile of these catalysts were validated and compared by filtration test and reaction progress, using the cross-coupling between 2-bromoanisole (**1**) and 4-fluorophenylboronic acid (**2**) initially as the model substrates, in an alcoholic solvent in the presence of K_3PO_4 (Figure 6). Using pristine catalysts, reactions were complete within 3 h at 75 °C. After cooling, the solution was filtered through standard laboratory filter paper (pore size 5-13 μm) to furnish clear,

colourless solutions (Figure 6, inset). A second batch of reactants, containing a different aryl bromide (4-bromoanisole, **4**), arylboronic acid **2** and base were added to the filtrate, and the mixture was reheated to 75 °C. In both cases, the formation of biaryl product **5** was observed within 2 h; confirming that leaching of catalytically active species occurs in both cases. However, while the reaction conducted in the filtrate obtained from Pd/ γ -Al₂O₃ was complete, only 22% conversion to the product was observed in the supernatant solution obtained from Pd EncatTM 30NP, confirming that the metal catalyst is more effectively retained by encapsulation.

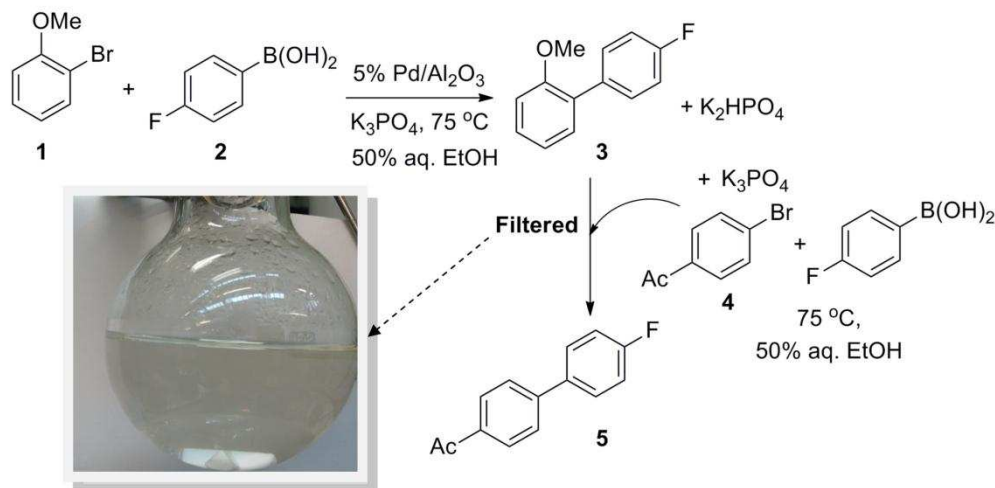


Figure 6. Chemical scheme for the filtration test. Inset: filtrate of the first reaction mixture.

The performance of the catalysts were also compared by reaction monitoring by HPLC, where it was found that the reaction catalysed by 4.5% Pd/ γ -Al₂O₃ (dried) was far more active, completed after 1 h, compare to 5 h required by the encapsulated catalyst (○ and ●, Figure 7). In accordance with previous reports,[12, 16] product formation followed a sigmoidal curve, indicative of the conversion of a precatalyst into an active catalyst at the beginning of the reaction. During this part of the study, it was found that pre-treatment of the catalysts with the reaction solvent (50% aq. ethanol) is detrimental to catalyst activity (◇ and ◆, Figure 7). In the case of Pd EncatTM 30NP, a very low conversion was obtained (<15% after 6 h).

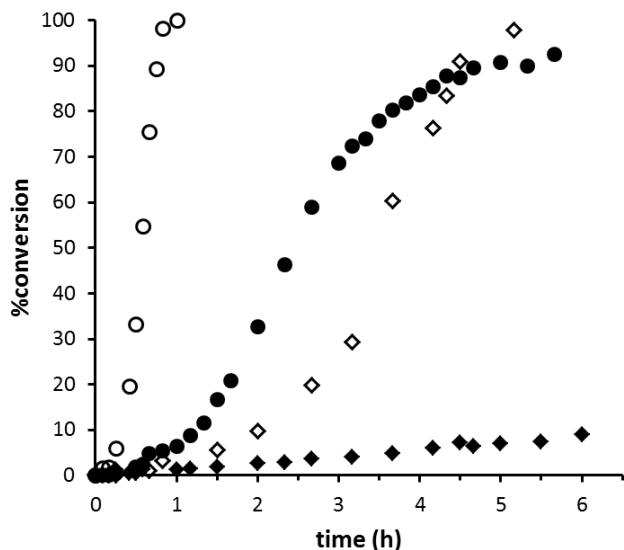


Figure 7. Catalytic activity of untreated ($\circ = 4.5\% \text{ Pd}/\gamma\text{-Al}_2\text{O}_3$, $\diamond = \text{Pd Encat}^{\text{TM}} 30\text{NP}$) and pre-treated ($\bullet = 4.5\% \text{ Pd}/\gamma\text{-Al}_2\text{O}_3$ (dried), $\blacklozenge = \text{Pd Encat}^{\text{TM}} 30\text{NP}$) catalysts.

3.3 Single-pass experiments.

Time-resolved catalytic activity was delineated by single-pass experiments, performed using the PFR described in Section 3.1. In the experiment, a mixture of reactants (aryl bromide **4**, aryl boronic acid **2** and K_3PO_4 in 50% aq. ethanol) was passed through a pre-heated catalyst cartridge at 75 °C. Aliquots of the eluent were collected at regulated intervals, which were analysed by HPLC to construct time-resolved reaction profiles (Figure 8). The residence time (τ) was kept deliberately short to afford low single-pass conversions (<10%), such that product inhibition may be eliminated.

Initially, reactions were performed by passing reaction mixtures through a pristine catalyst bed of Pd EncatTM 30NP. The result proved to be irreproducible^{**} (Figure 8A, data series in crosses), although a general trend may be observed, whereby an initial rapid increase in product formation was followed by a decay in productivity over time, converging towards a steady-state single-pass conversion at ca. 2.5%. Pre-treating the catalyst with a solution of aq. ethanol, by maintaining a steady solvent flow at 75 °C for 18 h, this inconsistency was removed; in this case, initial conversions were extremely low, but gradually increased over the timescale of the experiment with prolonged exposure to the reactants (Fig. 8A, \bullet). In contrast, similar pre-treatment of 4.5% Pd/ $\gamma\text{-Al}_2\text{O}_3$ (dried) by hot ethanol resulted in a different

^{**} The irreducibility may be due to the catalyst preparation process: Pd EncatTM 30NP catalyst is prepared by the reduction of the corresponding encapsulated palladium(II) acetate (Pd(II) EncatTM 30) with formic acid, so may contain varying amounts of Pd(II) salts

behaviour, whereby a very high conversion (nearly 8%) was observed initially, which decayed very rapidly towards a steady-state at ca. 1% (Fig. 8B, Δ).

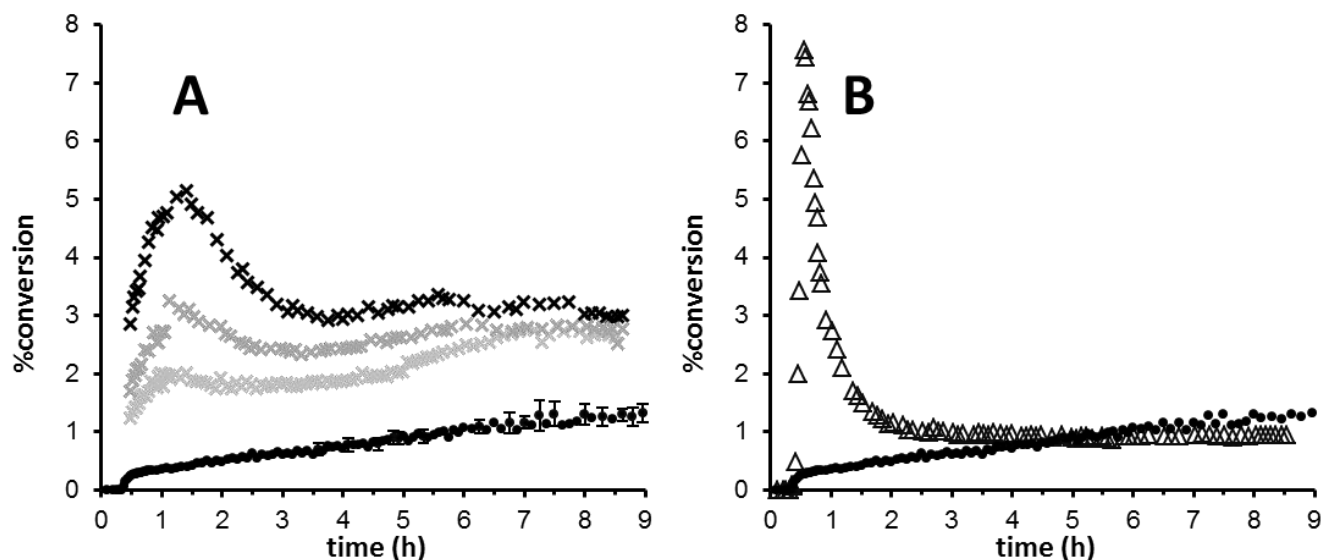


Figure 8. Single-pass conversions: **A** = Experiments performed with pristine (x) or pre-treated* (•) Pd EncatTM 30NP. **B** = experiments with pre-treated 4.5% Pd/ γ -Al₂O₃ (dried) (Δ) and Pd EncatTM 30NP (•). *average of two experiments, error bars are shown for errors greater than 0.1% conversion.

Comparing results in Figures 7 and 8, it is interesting to note that the ‘peak-and-decay’ behaviour observed for the untreated Pd EncatTM 30NP (Figure 8A, crosses) and treated 4.5% Pd/ γ -Al₂O₃ (dried) (Figure 8B, Δ) catalysts occur within the induction periods of the reactions (Figure 7, \diamond and •, respectively), whereas no induction period, or any notable catalyst activity, can be observed in its absence, as is the case for treated Pd EncatTM 30NP (Figure 8A, • and Figure 7, \blacklozenge). Thus, the ‘peak-and-decay’ feature is closely associated with the formation of catalytically active species, which is most likely due to leaching of Pd. Most importantly, these experiments provided the first direct evidence that catalyst activation and deactivation are dynamic processes, and that the reaction solvent (ethanol) affects the surfaces of these catalysts in different ways.

3.4 XAS studies.

To demonstrate the utility of the flow reactor in investigating the structural changes of Pd occurring within the catalyst bed, single pass experiments were performed at an X-ray absorption beam line (BM23, ESRF, Grenoble), where the reactor was mounted on a Huber motor. Spectra were recorded at a fixed position using a small vertically-focused X-ray beam, followed by mapping along the catalyst bed using QuEXAFS, moving the Huber motor in the z-direction.

3.4.1 Catalyst mapping. The catalyst bed can be located and positioned by measuring the absorption of X-ray at the Pd K-edge as the reactor was raised/lowered by the Huber motor (Figure 9). As the edge step can be directly related to the concentration of Pd in the catalyst bed, this can be used to track the movement of Pd species in the cartridge, i.e. leaching behaviour. Thus, a freshly-packed cartridge containing 8% Pd/ γ -Al₂O₃ (calcined) catalyst bed of ca. 3.6 mm in length exhibited well-defined boundaries of absorption that remained unchanged under a flow of cold solvent (Figure 9, ○). After treatment with hot ethanol for 2 h (Figure 9, x), catalyst leaching was visually detectable by the discolouration of the γ -Al₂O₃ packing above the catalyst bed (Figure 9A), corroborated by slight erosion of the signal intensity within region B (the catalyst bed) and the detection of Pd content above it in region C. Therefore, catalyst leaching occurs in the absence of reactants. After treatment with the reaction mixture (Figure 9, ◇), a slight redistribution of the Pd was observed along the direction of flow, from the entrance where reactants first come into contact with the catalyst, towards the middle of the bed (region B), i.e. leaching can also occur during the reaction. Similar results were obtained with a 4.5% Pd/ γ -Al₂O₃ (calcined) catalyst, demonstrating that the observed effect is not simply a function of metal loading. Redistribution was not observed with the Pd EncatTM 30NP catalyst over the equivalent timescale, which is not entirely unexpected, given that leaching from this catalyst is known to be low/slow.

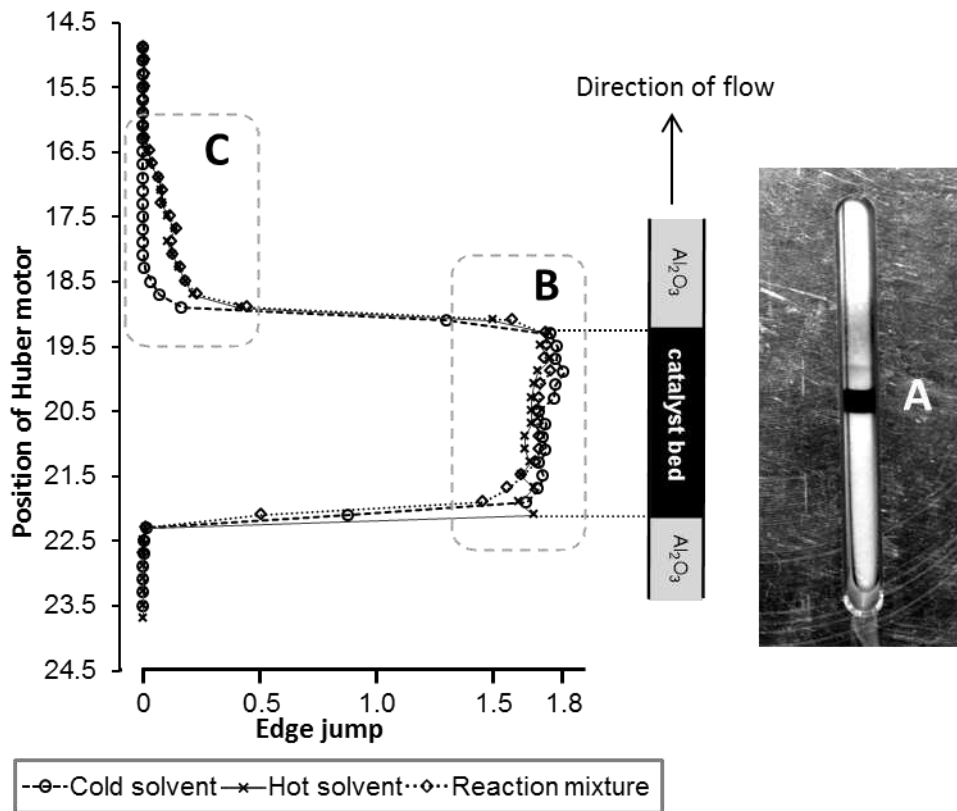


Figure 9. Mapping of 8% Pd/Al₂O₃ (calcined) catalyst bed before and after exposure to ethanol and reaction mixture. **A:** Visual indication of leaching. **B:** Catalyst bed region (between motor positions 22.1-18.5). **C:** γ -Alumina region (motor positions <18.5).

3.4.2 Reduction of Pd by EtOH in situ. Changes in the oxidation state of Pd can be detected by distinct changes in the white line of the Pd K-edge XANES spectra.[18] Fixing the X-ray beam at the entrance of the catalyst bed (Huber motor position 21.7), XAS spectra of 8% Pd/ γ -Al₂O₃ (calcined) were recorded initially under a flow of cold aqueous ethanol, before a temperature ramp was applied via the PID controller (26 to 75 °C). Pd/ γ -Al₂O₃ is known to exist in a partially oxidised PdO form when stored in air,[19] which was confirmed by comparing the Pd K-edge XANES spectrum of the prepared catalyst with palladium oxide. This appeared to be relatively stable in aqueous ethanol at ambient temperature, as no changes in the XANES region were observed. As the temperature increased, the reduction to Pd(0) was clearly observable, by the evolution of new maxima at 24370 and 24390 keV (Figure 10A). The same phenomenon was also observed for Pd EncatTM 30NP, which also appears to exist in a partially oxidised form and was reduced by hot aq. ethanol (Figure 10B).

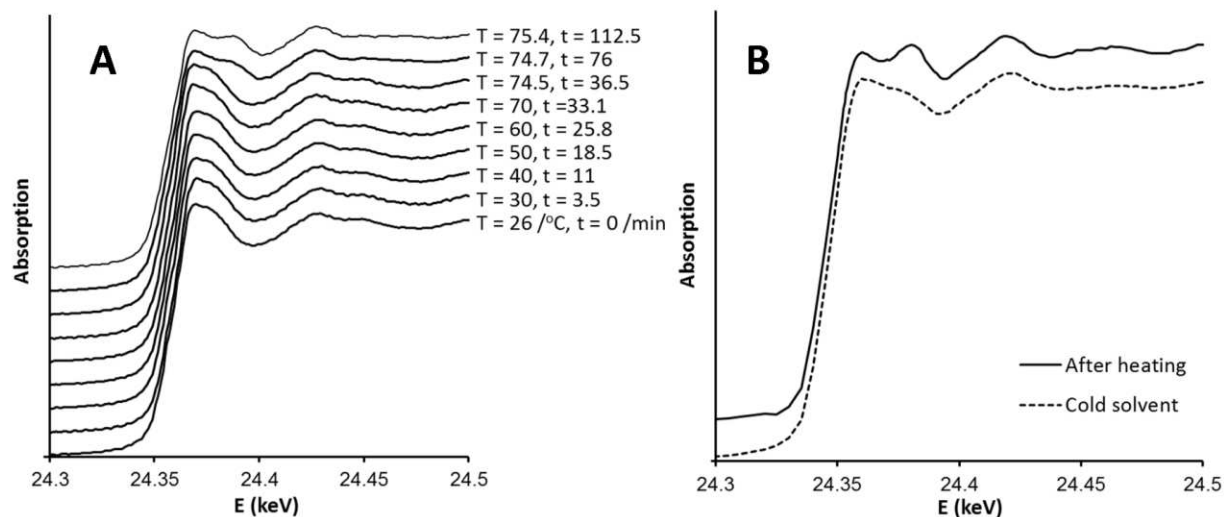


Figure 10. Reduction of Pd by hot ethanol. **A** = 8% Pd/ γ -Al₂O₃ (calcined); **B** = Pd EncatTM 30NP.

3.4.3 Speciation of Pd along the catalyst bed. Following each specific treatment with solvent or reaction mixture, the 8% Pd/ γ -Al₂O₃ (calcined) catalyst bed was mapped and longer scanning spectra recorded at specific points of interest within the bed. Remarkably, partitioning of Pd species was clearly observable along the catalyst bed after its exposure to hot ethanol (Figure 11A). Linear combination fitting of

reference spectra of a Pd foil and Pd oxide (Supplementary Material) shows the degree of reduction of the palladium at each point along the bed. Surprisingly, the entrance of the catalyst bed (position 21.7) where the solvent comes first into contact with the catalyst consisted mainly of Pd(II) (69% PdO : 31% Pd foil), while the exit of the catalyst bed (position 19.4) was dominated by Pd(0) species (73% Pd foil). XANES spectra were also recorded of the leached Pd species within the alumina bed (positions 18.5 and 16.7), which was found to consist mainly of Pd(0) species (70% and 59% Pd foil respectively). Subsequent treatment of the catalyst bed with the reaction mixture for an equivalent time period (2 h at 75 °C) affected only slight changes within the error of the analysis (Figure 11B).

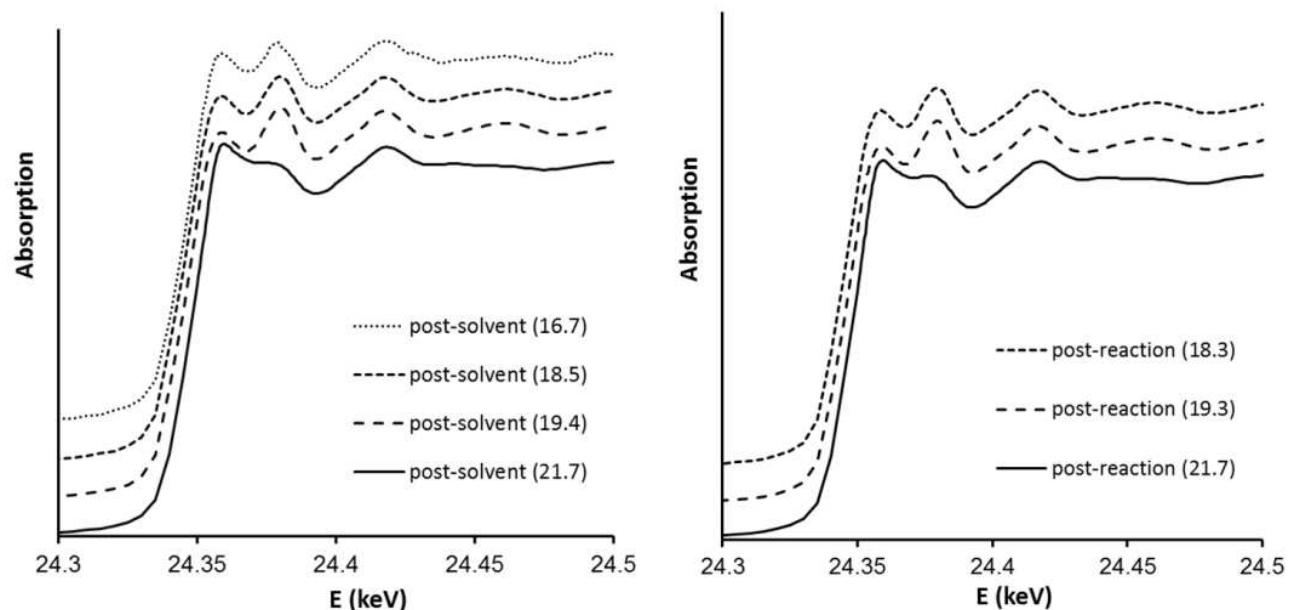


Figure 11. **A** = XANES spectra recorded at 4 positions in the catalyst bed (8% Pd/ γ -Al₂O₃ (calcined)) after exposure to ethanol at 75 °C for 2 h; **B** = XANES spectra recorded at 3 positions in the catalyst bed after exposure to reaction mixture (75 °C, 2 h). Positions of the Huber motor are indicated in parenthesis; refer to Figure 9 for corresponding axial positions within the catalyst bed.

The spatial resolution of the mapping experiments (see 3.4.1) is limited to 0.2 mm (the vertical size of the beam). Batch linear combination fitting of the mapping experiments showed increasing reduction though the first millimetre of the catalyst bed after which the ratio of Pd to PdO remained fairly constant (~70% Pd). Analysis of a comparable catalyst with lower loading, 4.5% Pd/ γ -Al₂O₃ (calcined) showed a similar pattern with increasing reduction over the first 0.6 mm of the catalyst bed, levelling off to approximately 75% Pd. Given that the entrance of the catalyst bed is expected to experience the greatest exposure to the solvent, it is not unreasonable to expect this region of the catalyst bed to undergo the largest amount of reduction (*i.e.* contain more Pd(0) species) – but this did not appear to be the case. This implies that palladium is not reduced by ethanol *per se* (pathway A, Figure 12), but by a by-

product of the reaction. An interesting possibility is the liberation of nascent H₂ during the process (pathway b, Figure 12), acting as the true reductant for PdO species further downstream.[20]

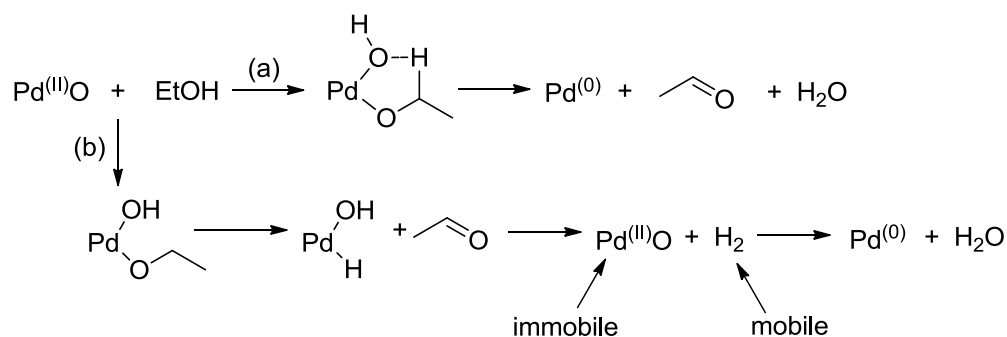


Figure 12. Two possible pathways for the reduction of palladium oxide by ethanol.

4. Conclusions

We have described the design, construction and characterisation of a plug flow reactor that is compatible with an X-ray absorption beam line, for time-resolved study of catalytic reactions. The reactor has been applied to monitor activation, deactivation and leaching behaviour of two catalysts (Pd/ γ -Al₂O₃ and Pd EncatTM 30NP) in the Suzuki-Miyaura cross-coupling reaction, revealing different reaction profiles. The reactor was subsequently deployed in an X-ray absorption beam line to examine structural changes of Pd, found to be strongly affected by the reaction solvent (ethanol) and the reaction mixture.

Interestingly, catalyst speciation along the bed was observed by EXAFS mapping, which revealed a highly unusual aspect of the redox chemistry of palladium with ethanol. More detailed examination of the EXAFS data are in progress, to identify the precise nature of the reduced form(s) of Pd species obtained, and these results will be presented elsewhere.

Corresponding Authors

*Dr. Klaus Hellgardt (Department of Chemical Engineering) and Dr. Mimi Hii (Department of Chemistry), Imperial College London, South Kensington, London SW7 2AZ, United Kingdom. Email: k.hellgardt@imperial.ac.uk; mimi.hii@imperial.ac.uk.

Present Addresses

†Current affiliation: School of Chemistry, University of Leeds, Woodhouse Lane, Leeds LS2 9JT, United Kingdom.

§Current affiliation: Departamento Química Inorgánica, Facultad de Química, Universidad de Santiago de Compostela, 15752, Santiago de Compostela, Spain.

ψCurrent affiliation: Brazilian Synchrotron Light Laboratory (LNLS), Laboratório Nacional de Luz Síncrotron, Caixa Postal 6192, CEP 13083-970, Campinas – SP, Brazil.

ACKNOWLEDGMENT

The work was funded by research grant: “Elucidate and Separate (ELSEP) - Palladium Catalysts in C-C and C-N Coupling Reactions (grant number: EP/G070172/1), with additional support from the Pharmacat Consortium (AstraZeneca, GlaxoSmithKline and Pfizer). LAA and EMB are supported by Xunta Galicia. We thank Johnson Matthey plc for the provision of Pd salts through an academic loan scheme, and ESRF for access to facilities. We are grateful to Mr. Stefanos Karapanagiotidis (Imperial College London) for his assistance with the construction of key electrical components of the reactor, and the thermal imaging experiment. Cl K edge and Pd L3 edge XANES were measured at the EPSRC-funded XMAS beamline at the ESRF. We are indebted to Paul Thompson and Didier Wermeille for their assistance in making these measurements.

References

- [1] A. Suzuki, *J. Synth. Org. Chem. Jpn.* 63 (2005) 312-324; S. Kotha, K. Lahiri, *Eur. J. Org. Chem.* (2007) 1221-1236; L. A. Adrio, J. M. Antelo Miguez, K.K. Hii, *Org. Prep. Proced. Int.* 41 (2009) 331-358; M. M. Heravi, E. Hashemi, *Monatsh. Chem.* 143 (2012) 861-880; R. Rossi, F. Bellina, M. Lessia, *Adv. Synth. Catal.* 354 (2012) 1181-1255.
- [2] Y. J. Deng, L. Z. Gong, A. Q. Mi, H. Liu, Y. Z. Jiang, *Synthesis* (2003) 337-339; J. M. Antelo Miguez, L. A. Adrio, A. Sousa-Pedrares, J. M. Vila, K. K. Hii, *J. Org. Chem.* 72 (2007) 7771-7774.
- [3] F. X. Felpin, T. Ayad, S. Mitra, *European J. Org. Chem.* (2006) 2679-2690; Y. Kitamura, A. Sakurai, T. Udzu, T. Maegawa, Y. Monguchi, H. Sajiki, *Tetrahedron* 63 (2007) 10596-10602; Y. Kitamura, S. Sako, T. Udzu, A. Tsutsui, T. Maegawa, Y. Monguchi, H. Sajiki, *Chem. Commun.* (2007) 5069-5071; Y. Kitamura, S. Sako, A. Tsutsui, Y. Monguchi, T. Maegawa, Y. Kitade, H. Sajiki, *Adv. Synth. Catal.* 352 (2010) 718-730; S.-Y. Liu, H.-Y. Li, M.-M. Shi, H. Jiang, X.-L. Hu, W.-Q. Li, L. Fu, H.-Z. Chen, *Macromolecules* 45 (2012) 9004-9009.
- [4] S. K. Beaumont, *J. Chem. Technol. Biotechnol.* 87 (2012) 595-600; M. Pagliaro, V. Pandarus, R. Ciriminna, F. Beland, P.D. Cara, *ChemCatChem* 4 (2012) 432-445; V. P. Ananikov, I. P. Beletskaya, *Organometallics* 31 (2012) 1595-1604; M. Pérez-Lorenzo, *J. Phys. Chem. Lett.* 3 (2011) 167-174.

- [5] A. F. Schmidt, A. A. Kurokhtina, *Kinet. Catal.* 53 (2012) 714-730; A. F. Schmidt, A. A. Kurokhtina, E.V. Larina, *Kinet. Catal.* 53 (2012) 84-90.
- [6] P. J. Ellis, I. J. S. Fairlamb, S. F. J. Hackett, K. Wilson, A. F. Lee, *Angew. Chem. Int. Ed.* 49 (2010) 1820-1824.
- [7] A. F. Lee, P. J. Ellis, I. J. S. Fairlamb, K. Wilson, *Dalton Trans.* 39 (2010) 10473-10482.
- [8] L. Shao, B. Zhang, W. Zhang, S.Y. Hong, R. Schlögl, D. S. Su, *Angew. Chem. Int. Ed.* 52 (2013) 2114-2117; Z. Niu, Q. Peng, Z. Zhuang, W. He, Y. Li, *Chem.–Eur. J.* 18 (2012) 9813-9817.
- [9] S. Reimann, J. Stötzel, R. Frahm, W. Kleist, J.-D. Grunwaldt, A. Baiker, *J. Am. Chem. Soc.* 133 (2011) 3921-3930.
- [10] B. R. Fingland, F. H. Ribeiro, J. T. Miller, *Catal. Lett.* 131 (2009) 1-6; S. Matam, O. Korsak, L. Bocher, D. Logvinovich, P. Hug, A. Weidenkaff, D. Ferri, *Top. Catal.* 54 (2011) 1213-1218.
- [11] S. K. Matam, M. H. Aguirre, A. Weidenkaff, D. Ferri, *J. Phys. Chem. C* 114 (2010) 9439-9443.
- [12] S. S. Soomro, F. L. Ansari, K. Chatziapostolou, K. Köhler, *J. Catal.* 273 (2010) 138-146.
- [13] C. Prestipino, O. Mathon, R. Hino, A. Beteva, S. Pascarelli, *J. Synchrotron Rad.* 18 (2011) 176-182.
- [14] C. Ramarao, S. V. Ley, S. C. Smith, I. M. Shirley, N. DeAlmeida, *Chem. Commun.* (2002) 1132-1133.
- [15] J. M. Richardson, C. W. Jones, *Adv. Synth. Catal.* 348 (2006) 1207-1216.
- [16] S. J. Broadwater, D. T. McQuade, *J. Org. Chem.* 71 (2006) 2131-2134.
- [17] R. K. Arvela, N. E. Leadbeater, M. S. Sangi, V. A. Williams, P. Granados, R. D. Singer, *J. Org. Chem.* 70 (2004) 161-168.
- [18] M. W. Tew, M. Nachtegaal, M. Janousch, T. Huthwelker, J. A. van Bokhoven, *Phys. Chem. Chem. Phys.* 14 (2012) 5761-5768.
- [19] S. F. J. Hackett, R. M. Brydson, M. H. Gass, I. Harvey, A. D. Newman, K. Wilson, A. F. Lee, *Angew. Chem. Int. Ed.* 46 (2007) 8593-8596.
- [20] The reduction of PdO by H₂ had been reported to occur by a dissociative chemisorption process, and is particularly facile on the PdO{101} surface: M. Blanco-Rey, D. J. Wales, S. J. Jenkins, *J. Phys.*

Chem. C 113 (2009) 16757-16765; C. Hakanoglu, J.M. Hawkins, A. Asthagiri, J.F. Weaver, J. Phys.
Chem. C 114 (2010) 11485-11497.